CRYSTAL GROWTH & DESIGN
2002
VOL. 2, NO. 5
431−435

Growth and Characterization of Doped TGS Crystals for Infrared Devices

Jiann-Min Chang, Ashok K. Batra, and Ravindra B. Lal*

Department of Physics, P. O. Box 71, Alabama A&M University, Normal, Alabama 35762, USA

Received May 2, 2002

ABSTRACT: Modified triglycine sulfate (TGS) single crystals have been grown from the aqueous solution by doping with urea, yttrium sulfate, L-serine + cobalt sulfate, and L-alanine + urea in the ferroelectric phase using a temperature lowering technique. The effects of these different dopants on the growth, dielectric, pyroelectric, optical, and mechanical properties have been investigated. TGS doped with urea and L-serine + cobalt sulfate exhibited higher material figures of merit for pyroelectric infrared detecting devices compared with pure TGS crystals. The Vicker's hardness studies at room temperature, carried out on (001) and (010) crystallographic planes using the Leitz Weitzler microhardness tester, show increased hardness of the doped crystals.

1. Introduction

Pyroelectric triglycine sulfate (TGS) crystals have technological importance[1] for room temperature infrared (IR) detectors, earth exploration, radiation monitoring, and astronomical telescopes. TGS is the best material among available materials as a sensitive element in pyroelectric sensors due to high pyroelectric coefficients, reasonably low dielectric constants, and best figures of merit.[1] Pyroelectric sensors based on TGS are uniformly sensitive to radiations in wavelength range from ultraviolet to far-infrared, and do not require cooling for operation as compared to quantum detectors, where low-temperature cooling is required. The crystal structure of TGS is monoclinic below the Curie temperature (49 °C). The space group transforms from P_{21} in the ferroelectric phase to cento-symmetrical P_{21}/m in the paraelectric phase. The b-cut/(010) crystals are used for detector fabrication, which is also a cleavage plane. Many efforts[1−17] have been made in the past to understand the growth mechanism and improve its pyroelectric, mechanical, optical, and ferroelectric properties, and to prevent depolarization[14] due to thermal, electrical, or mechanical means. Efforts are mainly focused toward understanding the growth mechanism and growth rate, and modifying the desired pyroelectric properties by doping TGS crystals with inorganic and organic dopants. TGS crystals have also been grown in the low gravity environment of space during NASA's Spacelab-3 and International Microgravity Laboratory-1 missions[18,19] to understand the growth mechanism and improve its IR detector characteristics and other properties. Metallic ions generally affect the morphology and growth rate of TGS crystals but do not improve the dielectric properties greatly. The metal ion dopants such as Cr, Cu, Fe, and Ni are incorporated isomorphically[13] in the form of metal glycino-chelates[9,13] with two molecules of glycine, thereby making the crystal lattice stronger. However, amino acids such as L-alanine and other dipolar organic dopants such as urea and nitro-anilines have been affective in reducing depolarization,[14] and in increasing the pyroelectric figures of merit,[1] which are essential material parameters for determining their use in IR detector applications. However, TGS crystals doped with L-alanine show a tendency to fragility[15] and breakage when samples were prepared in the form of extremely thin elements for use in IR detectors. The improved yield and pyroelectric properties were also observed in pure TGS crystals grown on poled seeds.[16]

In light of research work done on doped TGS crystals, we thought it interesting to study the effects of doping simultaneously with L-alanine + urea (organic dipolar molecules), Co + L-serine (transition metal ion and dipolar organic molecule respectively), yttrium (rare earth ion), and urea (dipolar organic molecule) on growth rate, growth yield, morphology, and dielectric, optical and pyroelectric and mechanical properties of TGS crystals in the present work. Using these properties/parameters, applicable materials figures of merit of doped TGS crystals for their use in IR detectors and vidicons are calculated for comparison over pure TGS crystals.

2. Experimental Methods

2.1. Growth of Crystals. Single crystals of pure and doped TGS were grown by a temperature lowering method using a modified version of the crystallization equipment shown in Figure 1. A 15-L Plexiglas main tank of crystallizer is provided with a Plexiglas cover which holds a 4 × 4 × 4 in. crystallization cell, heating elements, and temperature sensors. The slotted iron frame holds the two stirrers and seed holder motor. The reciprocating motion of seed holder is controlled by an electronic controller, designed and fabricated in our laboratory.[1] About half-inch diameter thin walled plastic balls are floated on the surface of water in the outer tank to minimize the evaporation of water. The evaporation of TGS solution in the crystallization cell along the seed holder rod is minimized by a water seal designed by us. The saturated solution of pure and doped TGS at 40 °C was prepared in deionized water using BDH chemicals Optran grade TGS crystalline powder. The concentration of dopants as presented in Table 1 is calculated according to TGS solution. The growth solutions were equilibrated in the crystallization cell at 42 °C for 24 h. The temperature of the crystallizer was maintained within 0.01 °C using YSI 72 proportional temperature controller. The appropriate and good quality polyhedral TGS and doped TGS

* To whom correspondence should be addressed. Tel.: 256 858-8148 Fax.: 256 851-5622 E-mail: rlal@aamu.edu.

10.1021/cg020018g CCC: $22.00
Published on Web 08/07/2002

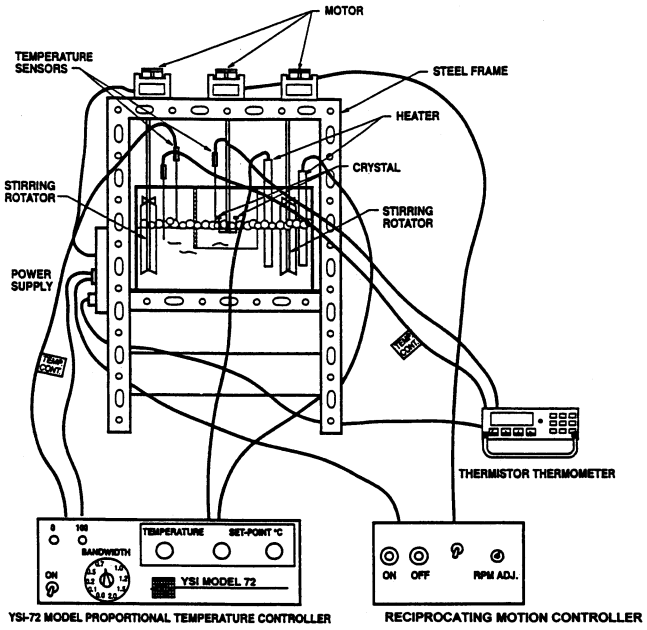

Figure 1. Schematic diagram of the crystal growth setup.

seed crystals were grown by the slow evaporation technique, and were fixed on seed holder spikes with Dow Corning 732 silicon 2 adhesive. The dimensions of the seeds along the [010] and [001] directions were measured and recorded along with mass of the seeds. The seed holder and the seed crystals were preheated to 42 °C before insertion into the growth cell to avoid thermal shock to the seeds. The seed crystals were allowed to dissolve slightly before the temperature was lowered to the correct saturation temperature, and then held for 24 h. The Schilleren technique[17] was used to check the correct saturation temperature by observing growing or dissolving plume of concentration gradients. Afterward, the solution temperature was lowered at a programmed rate that decreased from initial 0.2 °C per day to 0.5 °C per day. All other growth parameters such as stirring rate, temperature of growth, and temperature lowering rate were kept identical for all crystal growth experiments so as to balance out their effects on the properties of resulting crystals. After completion of the growth run, the crystals were removed from the solution and slowly cooled to room temperature in a special oven to avoid any thermal shock. Transparent and good optical quality crystals were generally obtained.

2.2. Crystal Characterization. (a) Crystal Morphology and Growth Rate. The three dimensional view of the pure crystals and doped crystals was obtained from goniometric measurements as shown in Figure 2. The growth rate (axial velocity) and growth yield were calculated by measuring the seed crystals and grown crystals dimensions and mass, respectively, using the following formulas:

$$V = (d_c - d_s)/\Delta T \cdot T$$

where V is the axial growth rate, d_c is the axial dimension of grown crystal, d_s is the axial dimension of seed crystal, ΔT is the amount of undercooling, and T is the time of growth.

$$R = (W_c - W_s)/\Delta T \cdot T$$

where R is the growth yield, W_c is the mass of crystals grown, W_s is the mass of seed crystals, ΔT is the amount of undercooling, and T is the time of growth.

(b) Fourier Transforms Infrared (FTIR) Measurements. The infrared spectra were taken using the Perkin-Elmer model 1725X Fourier transform infrared (FTIR) spectrometer using a microscopic attachment. All samples were crushed to a fine powder and mixed with KBr powder to obtain IR spectra at room temperature.

(c) Dielectric and Pyroelctric Properties. In this study, the slice of each sample was cleaved perpendicular to (010) axis (ferroelctric axis) of pure and doped crystals. The cleaved specimens of size 5 × 5 × 0.5 mm were lapped and polished using fine grit 3−5 micron alumina polishing paper and isopropyl alcohol as lubricant. The polished surfaces were examined under an optical microscope for any induced defects, and finally polished by water and tetra-chloroethylene to remove any polishing residue. Before thermally evaporating silver electrodes, the samples were cleaned ultrasonically. After applying the electrodes and before the electrical measurements, the samples were kept at 60 °C for 48 h to remove any moisture present. The dielectric permittivity were calculated by measuring capacitance at frequency of 1 kHz at an applied signal field of 10 V/cm using GenRad 1620AP capacitance measuring assembly in a three-terminal cell designed in our laboratory. The pyroelectric current was measured using the Byer and Roundy method,[20] and the pyroelectric coefficient (P) was calculated using the relationship:

$$P = (I/A)/(\mathrm{d}T/\mathrm{d}t)$$

where I is the current, A is the area of electrodes, and $\mathrm{d}T/\mathrm{d}t$ is the rate of change of temperature. Using the above parameters, the following material figures of merit[1] for accessing the characteristics of single element pyroelectric detector, operating in an optimum manner, were calculated for comparison:

$F_i = P$ for high current responsivity,

$F_v = P/\epsilon'$ for high voltage responsivity, and

$F_{vid} = P/\sqrt{\epsilon'}$ for vidicon applications,

where P is the pyroelectric coefficient and ϵ' is the dielectric constant.

(d) Microhardness Measurements. The microhardness measurements were made using the Leitz Wetzler hardness tester with Vicker's diamond pyramidal indentor. Selected surfaces of (001) and (010) faces of pure and doped crystals were subjected to Vicker's static indentation for a load of 0.49 N for a dwell time of 15 s. The hardness number was estimated from the relationship:

$$H_v = 1.81544p/d^2 \ (\mathrm{g/micron^2})$$

where H_v is the Vicker's microhardness, p is the applied force, and d is the diagonal length of the indentation impression.

3. Results and Discussion

Figure 2 and Table 1 show the morphology and average growth data of pure and doped TGS crystals, respectively. It can be inferred that presence of dopants in the process of crystal growth results in changes in growth rates along [001] and [010] directions and growth yield, and hence the modification in the crystals habits as depicted in Figure 2. The growth is anisotropic in nature. It is relatively higher along [010] directions than the [001] direction, thereby we observed smaller (010) as compared with (001) faces in both pure and doped TGS crystals. The lower growth rate of the (001) face shows that the growth is energetically more difficult on these faces, and crystallization is probably, in our case, limited by the process of stacking of growth units on the crystal surfaces. It is well-known that when a solute crystallizes from its supersaturated solution, the presence of impurities can often have a great effect on the growth kinetics and the habit of crystalline phase.[1,21] The impurities exhibit a marked specificity in their action as they are absorbed onto the growing crystal. Surface absorption of impurities onto crystal faces changes the relative surface free energies of the face, blocks sites essential to incorporation of new solute molecules into the crystal lattice, and hence slows the

Table 1. Growth Data of Pure and Doped TGS Crystals

crystals	dopants	normalized growth yield (g/d/°C)	axial growth velocity (mm/d/°C)		
			$V_{[010]}$	$V_{[001]}$	$V_{[010]}/V_{[001]}$
TGS	pure	0.12	0.218	0.061	3.57
5% UrTGS	5 wt % urea	0.604	0.767	0.251	3.06
UrL-ATGS	5 wt % urea + 5 wt % L-alanine	0.227	0.403	0.187	2.16
L-sCoTGS	5 wt % L-serine + 1 wt % cobalt sulfate	0.475	0.483	0.232	2.08
YTGS	3 wt % yttrium sulfate	0.384	0.393	0.188	2.09

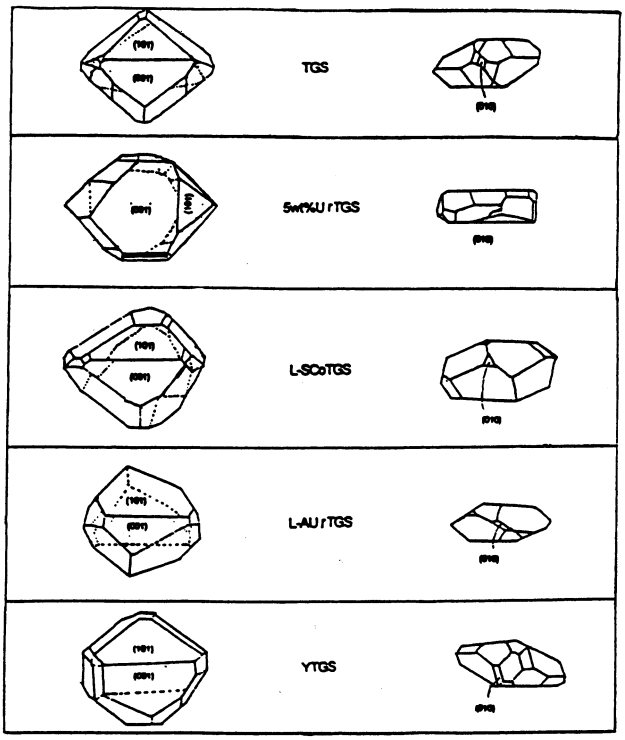

Figure 2. Morphology of pure and doped TGS crystals.

growth. However, the decrease in growth rate is generally explained in the literature[22] on the basis of kinetic theory, i.e., the impurities absorbed on the crystal surface impede the movement of steps by different mechanisms depending on the site of absorption such as adsorption on ledges or between steps. In our crystal system studied, it is not possible to give a concrete explanation for the increase in growth without the determination of free surface energy as a decrease in the surface energy increases the growth rate of crystal faces. Furthermore, crystal growth in the presence of impurities is a very complicated process, and there are many possible reasons for the observed effect. In the crystal system studied, L-alanine, urea, and serine are organic compounds and may replace the glycine molecule during growth, while metal ions form metal−glycine complexes that are possibly stereochemically similar to a part of TGS lattice so that they could replace glycine II, glycine III, and two adjacent sulfate ions, whereas Co (II) is situated in an interstitial position between glycine II and III. It may be pointed out that there are three glycine molecules per unit cell of TGS. It can be reasonably said that structure and type of metal complexes formed in the TGS lattice will determine the growth rate and hence the crystal habit. Table 2 shows the values obtained for dielectric constant, pyroelectric coefficient, and calculated material figures of merit for pure and doped crystals at various temperatures. The pyroelectric coefficient and dielectric constant for UrL-ATGS and YTGS crystal have decreased, whereas they have increased for the 5% UrTGS and L-SCoTGS crystals as compared with pure TGS crystals. The increase in the pyroelectric coefficient is attractive for their use in pyroelectric infrared detector applications. The values of pyroelectric coefficient in doped TGS crystal depend on the site of their incorporation, chemical nature of dopants (dipole moment, etc.) complex formed with glycine molecules (polar glycine), and other factors such as the charge displacement in the cell and around the doped cells. However, in the TGS crystal, which is ferroelectric, the values of the dielectric constant and pyroelectric coefficient depend on the domain structure (frittering of domains or single domain) and dynamics, type of defects (polar or nonpolar) formed in the crystal cell due to doping, direction of polarity of defect formed, and the dipole interaction of the impurity defects and the host. It is noteworthy to mention that single domain TGS crystals have higher pyroelectric coefficient and lower dielectric constant as compared with multi or pinned domain crystals. It can therefore be said that urea and L-serine + codopants might be producing single domain crystals, while urea, L-alanine, and yttrium dopants might be producing multi or pinned domain crystals.

Figures 3−7 show the FTIR spectra of pure and doped TGS crystals. The NH, OH, and CH absorptions are smeared into a continuum that occurs around 1700 cm^{-1}. The absorption around 1700 cm^{-1} (Figure 3) is due to C═O stretching of the -COOH group. The strong absorption around 1050 cm^{-1} is due to the sulfate part of the TGS molecules. The strong peak at 2400 cm^{-1} is due to CO_2 in the atmosphere. The 5% UrTGS crystal has significantly better transmission (Figure 4) over the measurable range studied. Figures 5 and 6 show that L-SCoTGS and UrL-ATGS are two different kinds of dopant, and hence their FTIR spectra are drastically changed from the pure TGS crystal. The FTIR spectra of YTGS crystals (Figure 7) show the NH absorption peak at 3200 cm^{-1}, which is stronger than pure TGS crystal.

The results of Vicker's hardness measurements for pure and doped TGS crystals are given in Table 3. In case of pure TGS crystal, the hardness of the (001) face is greater than the (010) face, implying that the (001) crystallographic plane is closely packed. The hardness of doped crystals is increased along the (001) and (010) cleavage plane. However, the increase in hardness of the (001) plane in doped crystals is not very significant when compared with pure TGS crystal. Hardness of a material is a measurement of the resistance it offers to local deformation. The extent to which a material will deform plastically under an applied stress depends on the strength of intermolecular forces that are broken and connected in the process of doping. The large increase in the hardness of doped crystal studied along

Table 2. Figures of Merit of Pure and Doped TGS Crystals

crystals	temp (°C)	ϵ'	P (nC/(cm)^2 °C)	F_i (nC/(cm)^2 °C)	F_v (nC/(cm)^2 °C)	F_{vid} (nC/(cm)^2 °C)
TGS	35	70	45	45	0.64	5.4
	40	105	80	80	0.75	7.8
	45	250	160	160	0.64	10
5% UrTGS	35	92.7	240.5	240.5	2.59	24.97
	40	143	321.7	321.7	2.25	26.88
	45	423	384.2	384.2	0.91	18.69
UrL-ATGS	35	38.9	44.57	44.57	1.15	7.14
	40	57.8	59.42	59.42	1.03	7.82
	45	112	145.65	145.65	1.3	13.77
L-sCoTGS	35	72.7	285.4	285.4	3.92	33.47
	40	114	327.7	327.7	2.87	30.64
	45	314	558.8	558.8	1.78	31.55
YTGS	35	6.7	2.517	2.517	0.37	0.97
	40	10.9	2.74	2.74	0.25	0.83
	45	29	12.74	12.74	0.44	2.37

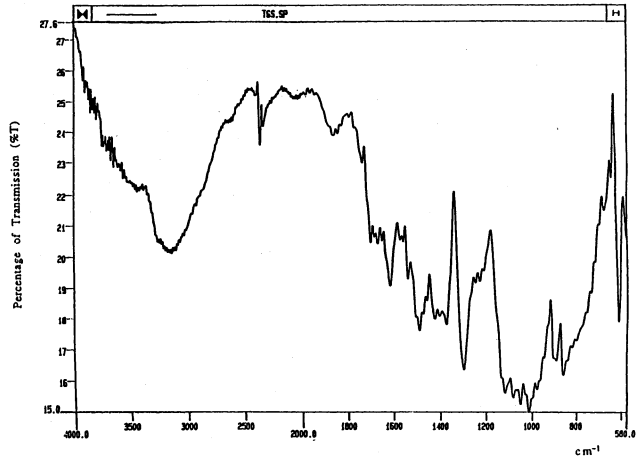

Figure 3. FT-IR spectra of pure TGS crystal.

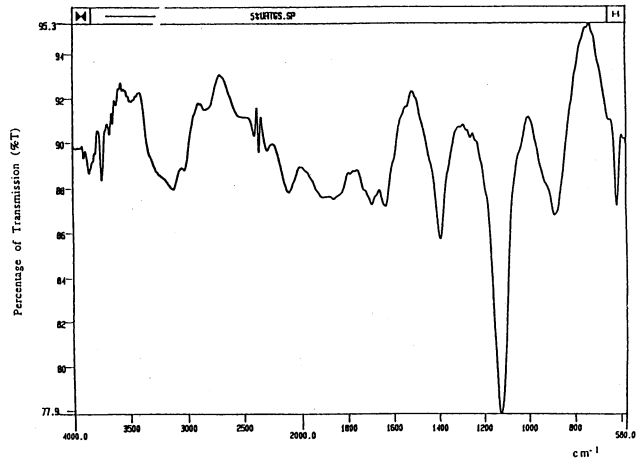

Figure 4. FT-IR spectra of 5% UrTGS crystal.

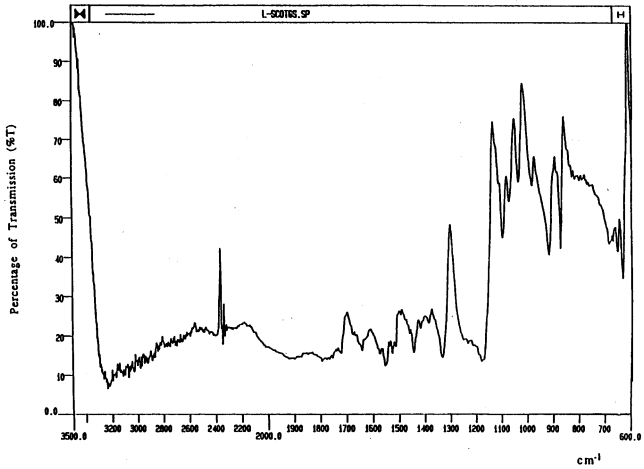

Figure 5. FT-IR spectra of L-SCoTGS crystal.

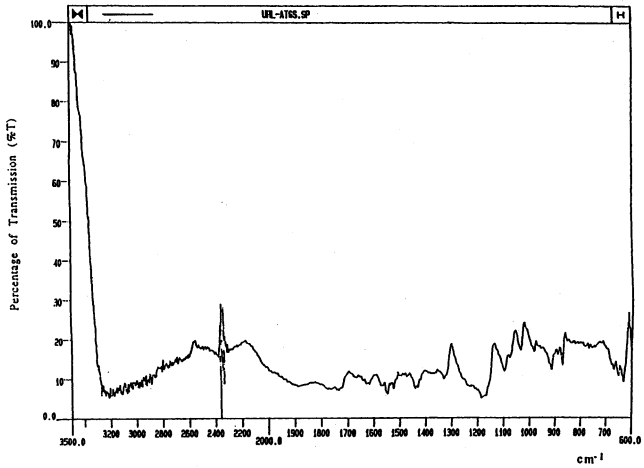

Figure 6. FT-IR spectra of UrL-ATGS crystal.

(010) plane can be attributed to the fact the doped molecules on incorporation into the TGS lattice enhances the strength of the bonding with the host molecule. It is noteworthy to mention that an increase in the hardness will have significant effect on IR detector element fabrication and processing such as ease in polishing, and less wastage due to cracking/breakage while polishing, etc.

4. Conclusions

The experimental results of the present investigation of doped TGS crystal system can be summarized as follows, comparing with pure TGS crystals:

(i) The crystal morphology of various doped crystals studied is essentially the same as undoped crystals.

(ii) The normalized value of growth velocity ratio V_{010}/V_{001} is modified as compared with pure TGS crystal.

(iii) The normalized growth yield is increased about six times in doped 5% UrTGS crystals in comparison with pure TGS crystals.

(iv) The pyroelectric coefficient of 5% UrTGS and L-SCoTGS crystals is higher than that of pure TGS crystals, which makes them superior for using them in infrared detecting devices.

(v) The calculated material figure of merit for high current responsivity (F_i) is higher for 5% UrTGS and

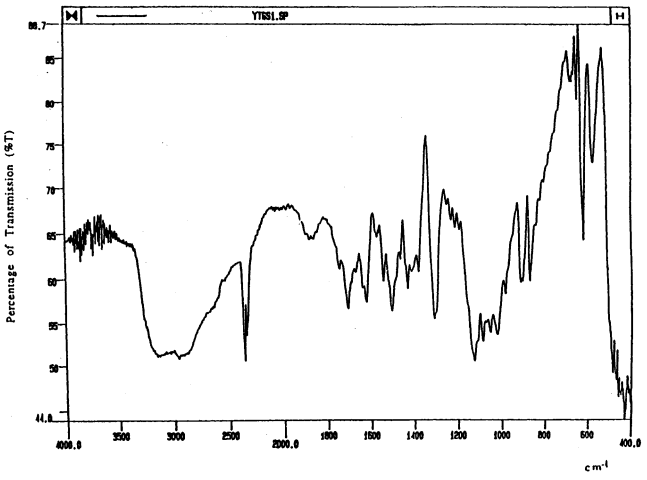

Figure 7. FT-IR spectra of YTGS crystal.

Table 3. Microhardness of Pure and Doped TGS Crystals

	Vicker's hardness number g/(μm)^2	
crystals	{0 0 1}	{0 1 0}
TGS	102.78	89
5% UrTGS	123.8	178.2
L-sCoTGS	233.2	273
Url-ATGS	159.2	217.2
YTGS	215.4	251.2

L-SCoTGS crystals; however, it is decreased for UrL-ATGS and YTGS crystals. The figure of merit for high voltage responsivity (F_v) and for vidicon application (F_{vid}) is higher for doped TGS crystals studied except YTGS crystals in the temperature range of 35−45 °C.

(vi) There is an increase in Vicker's hardness along the (001) and (010) crystallographic planes for doped TGS crystals, while the increase is significantly greater for the (010) planes. Doped crystals do not crack while lapping and polishing down to extremely thin slices for use in IR devices.

Summarizing, the 5% UrTGS and L-SCoTGS crystals grown during this study have been shown to possess superior properties such as materials figures of merit, growth yield, and microhardness over pure TGS crystals, and are therefore, very useful for IR detecting device applications.

Acknowledgment. The authors wish to acknowledge the support from the Office of Commercial Programs, National Aeronautics and Space Administration, Washington, DC, for a grant through the Center of Commercial Development of Space, Clarkson University, Potsdam, NY.

References

(1) Lal, R. B.; Batra, A. K. *Ferroelectrics* **1993**, *142*, 51−82.
(2) Gaffar, M. A.; Al-Fadl, A. A. *Cryst. Res. Technol.* **1999**, *34*(7), 915−923.
(3) Sun, D.; Yu, X.; Gu, Q. *Cryst. Res. Technol.* **1999**, *34*(10), 1255−1263.
(4) Prokopova, L.; Novotny, J.; Micka, Z.; Mailina, V. *Cryst. Res. Technol.* **2001**, *36*(11), 1189−1195.
(5) Aravazhi, S.; Jayavel, R.; Subramanium, C. *Mater. Res. Bull.* **1997**, *32*(11), 1503−1513.
(6) Meera, K.; Aravazhi, S.; Raghavan, P. S.; Ramasamy, P. *J. Cryst. Growth* **2000**, *221*, 220−240.
(7) Mathur, S. C.; Batra, A. K.; Mansingh, A. *J. Phys. D: Appl. Phys.* **1980**, *13*, 79−83.
(8) Gaffar, M. A.; Al-Fadl, A. A.; Mansour, S. A. *J. Phys. D: Appl. Phys.* **1999**, *34*(7), 915−920.
(9) Ramos, S.; Cerro, J. D.; Martin, J. M.; Brezina, B.; Havrankova, M. *Ferroelectrics* **1994**, *157*, 293−297.
(10) Chang, Jiann-Min.; Batra, A. K.; Lal, R. B. *J. Cryst. Growth* **1996**, *158*, 284−288.
(11) Sun, X.; Wang, M.; Pan, Q. W.; Shi, W.; Fang, C. S. *Cryst. Res. Technol.* **1999**, *34*(10), 1251−1254.
(12) Banan, M.; Lal, R. B.; Batra, A. K. *J. Mater. Sci.* **1992**, *27*, 2291−2297.
(13) Moravec, F.; Novotny, J. *Kristall Technik.* **1971**, *6*(3), 335−342.
(14) Bye, K. L.; Whipps, P. W.; Keve, E. T. *Ferroelectrics* **1972**, *4*, 253−256.
(15) Hotska, V. L.; Holakovsky, J.; Fousek, J.; Brezina, B. *Cryst. Res. Technol.* **1989**, *24*(1), 91−95.
(16) Banan, M.; Lal, R. B.; Batra, A. K.; Aggarwal, M. D. *Cryst. Res. Technol.* **1989**, *24*(3), 53−55.
(17) Lal, R. B.; Batra, A. K.; Aggarwal, M. D.; Kroes, R. *NASA Final Tech. Rep.* 1987, NAS8-32945.
(18) Lal, R. B.; Batra, A. K.; Trolinger, J. D.; Wilcox, W. R. *Microgravity Q.* **1994**, *4*(3), 186−198.
(19) Lal, R. B.; Batra, A. K.; Aggarwal, M. D.; Kroes, R.; Wilcox, W. R.; Trolinger, J. R.; Cirino, P. *NASA Conf. Publ.* **1987**, *2429*, 255−263.
(20) Byer, R. L.; Roundy, C. B. *Ferroelectrics* **1972**, *3*, 333−338.
(21) Davey, R. J. *J. Cryst. Growth* **1976**, *34*, 109−119.
(22) Sangwal, K.; Mielniczek-Brzoska, E. *Cryst. Res. Technol.* **2001**, *36*, 837−849.

CG020018G